9th AUSTRALASIAN
FLUID MECHANICS CONFERENCE,
AUCKLAND, 8-12 DECEMBER 1986

Waves due to Vehicles on Floating Ice Sheets

R. J. HOSKING and A. D. SNEYD

Department of Mathematics, University of Waikato, Hamilton, New Zealand.

ABSTRACT

A fast vehicle such as a landing aircraft generates flexural waves in floating ice over which it moves. The pattern of these elastic-gravity waves depends on the source speed, including the existence of caustics and the emergence of a shadow zone behind the source at high speed. At low speed the flexural response becomes static rather than wavelike- but there can then be slower internal waves in the underlying water if it is stratified. The amplitude, frequency and phase of the flexural waves also depend on the thickness and elastic properties of the ice. The internal waves may produce significant drag at rather low vehicle speed. We assume an impulsively-started source to show that the gravity-dominated flexural waves behind the source evolve relatively slowly, and finally we compare our theory with extensive recent empirical work.

1. INTRODUCTION

The sea-ice cover in McMurdo Sound (Antarctica) has been used as an aircraft runway since the International Geophysical Year (1957/8). Increased air pressure immediately below a landing aircraft constitutes a moving load that generates flexural waves in the ice (Davys et al. 1985). Earlier authors were especially interested in a critical speed at which a moving load produces a magnified response in the ice, in order to predict fracture (Nevel 1970; Kheisin 1971; Eyre 1977; Beltaos 1981). Hovercraft exploiting this phenomenon are being used as ice breakers on the Saint Lawrence Seaway in Canada, but at McMurdo Sound the United States Air Force intends to avoid it! Rather, an objective could be to monitor ice strength from the flexural waves generated, using instruments placed on the ice.

A reasonable mathematical model is an elastic homogeneous ice plate of infinite extent, resting on incompressible inviscid fluid of constant depth. The dispersion relation for plane waves in this system was given almost 100 years ago by Greenhill (1887), and is discussed in the next section. We also consider the possibility that the underlying fluid is stratified, when internal waves can be generated. The wave patterns generated by a steadily-moving source are then discussed, followed by further detailed consideration of the theoretical response for comparison with experiment.

2. FLEXURAL WAVES

We consider an extensive homogeneous ice sheet of thickness h and density ρ_i floating on water of finite depth and density ρ (c.f. figure 1). If $\eta(x,y,t)$ denotes a small vertical deflection, the equation of motion of the ice sheet is

$$D\nabla^4\eta + \rho_i h\eta_{tt} = p - f(x,y,t) \ ,$$

where the modulus of rigidity $D = \frac{1}{12}Eh^3/(1-\nu^2)$ is sensitive to the ice thickness h, p represents the restoring water pressure on the ice, and $f(x,y,t)$ is the downward stress on the ice due to the vehicle. The sea water flow will be approximately irrotational, with velocity potential ϕ, so Bernoulli's theorem gives

$$p = -\rho(\phi_t)_{z=0} - \rho g\eta \ .$$

The dispersion relation for uniform plane waves ($\eta \sim \exp[i(kx - \omega t)]$) obtained when $f = 0$ is thus

$$\omega^2 = \frac{Dk^5/\rho + gk}{kh' + \mu} \ , \qquad h' = \rho_i h/\rho$$

When density variations in the sea water are negligible, $\mu \to \coth kH$. Typical curves for the phase speed $c = \omega/k$ and the group speed $c_g = d\omega/dk$ for *flexural* waves in the ice are shown in figure 2. For stratified water μ depends on the frequency ω, when there are also slow *internal* waves propagating in the water - c.f. Section 3.

There are three important lengthscales associated with this dispersion relation (Davys et al. 1985) - viz. a short scale characterised by the (modified) ice thickness h'; a long scale characterised by the water depth H; and an intermediate scale characterised by the reciprocal of the wavenumber k_{min} at which the phase speed is a minimum (c_{min}), and where the effects of ice elasticity and gravity are comparable. For very short waves where $kh' \gtrsim O(1)$

$$\omega^2 \approx \frac{D}{h'\rho}k^4$$

and the group speed is twice the phase speed, so elastic-dominated flexural waves appear ahead of the moving source. Otherwise we may neglect the ice acceleration term in the equation of motion, so provided water stratification is also neglected the dispersion relation can be approximated by

$$\omega^2 = \left(\frac{Dk^4}{\rho g} + 1\right)gk\tanh kH \ .$$

For long waves where $kH \lesssim O(1)$ we have

$$\omega^2 \approx gk\tanh kH \ ,$$

which is the familiar dispersion relation for gravity waves on water of depth H, with group speed less than phase speed so gravity-dominated flexural waves appear behind the source. Since $k_{min}h' \ll 1$ and $k_{min}H \gg 1$, the approximate dispersion relation for waves of intermediate length is

$$\omega^2 \approx \frac{Dk^5}{\rho} + gk \ ,$$

and the minimum phase speed is thereby identified as

$$c_{min} \approx 2\left(\frac{Dg^3}{27\rho}\right)^{1/8}$$

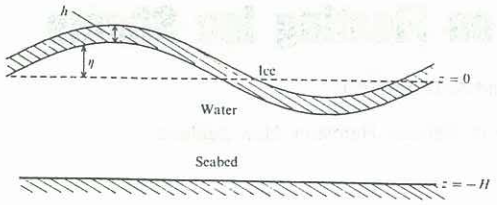

Figure 1. Diagram of floating ice plate.

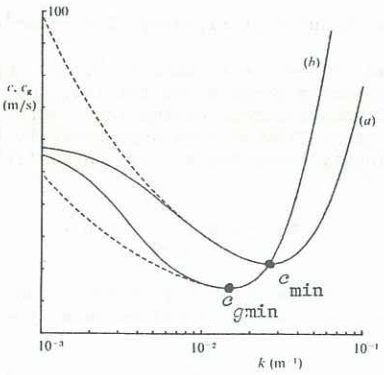

Figure 2. Graphs of phase speed (a) and group speed (b) against wavenumber k. The solid curves are for water of depth 350 m and the dashed curves for water of infinite depth. Note that the wavenumber scale is logarithmic. ($E = 5 \times 10^9 N/m^2$, $h = 2.5$ m, $\nu = \frac{1}{3}$.)

3. INTERNAL WAVES

Stratification of the water beneath the ice can be seasonal, and fresh water from the land may overlay the denser sea water in estuaries or fiords (Lewis and Walker 1970; Lamb 1945). If we adopt a simple two-layer model, with a layer of density ρ_1 and depth H_1 above a layer of density ρ_2 extending to a total depth H_2, we obtain (Schulkes et al. 1986):

$$\mu(\omega) = \coth kH \frac{\rho_1 \tanh kH_1 + \rho_2 \coth k(H_2-H_1) - gk(\rho_2-\rho_1)/\omega^2}{\rho_1 \coth kH_1 + \rho_2 \coth k(H_2-H_1) - gk(\rho_2-\rho_1)/\omega^2}$$

hence the dispersion relation is a quartic with quadratic roots

$$\omega_\pm^2 = \frac{Q \pm \sqrt{Q^2 - 4PR}}{2P},$$

where writing $\lambda = 1 + Dk^4/(\rho_1 g)$ we have

$$P = \rho_1 + \rho_2 \coth kH_1 \coth k(H_2-H_1) + kh'[\rho_1 \coth kH_1 + \rho_2 \coth k(H_2-H_1)],$$

$$Q = gk[(\rho_2-\rho_1)\coth kH_1 + \lambda(\rho_1 \coth kH_1 + \rho_2 \coth k(H_2-H_1)) + kh'(\rho_2-\rho_1)],$$

$$R = g^2k^2(\rho_2-\rho_1)\lambda.$$

There are now virtually two degrees of freedom, with flexural waves near the surface $z = 0$ but also internal waves in the neighbourhood of the interface $z = -H_1$ (c.f. Lamb 1945). For very short waves where $kh' \gtrsim O(1)$, we recover the classical dispersion relation for internal gravity waves at the interface of two superposed fluids of infinite extent - viz.

$$\omega_-^2 \approx gk(\rho_2-\rho_1)/(\rho_2+\rho_1);$$

and for long waves where $kH_2 \lesssim O(1)$ we find

$$\omega_-^2 \approx gk(1-\rho_1/\rho_2)[\coth kH_1 + \coth k(H_2-H_1)]^{-1}.$$

The stronger elastic-gravity hybrid character of the flexural waves is evident from the respective approximate quadratic roots for waves of intermediate length, certainly greater than the depth of the stratification but less than the total depth ($kH_1 = O(1)$ but $kH_2 \gg 1$):

$$\omega_+^2 \approx \frac{Dk^5}{\rho_1}\,\frac{\rho_1 \coth kH_1 + \rho_2}{\rho_2 \coth kH_1 + \rho_1} + gk\,\frac{1 + \coth kH_1}{\rho_1/\rho_2 + \coth kH_1},$$

$$\omega_-^2 \approx gk(1 - \rho_1/\rho_2)\left[1 + \frac{gk + Dk^5/\rho_2}{gk + Dk^5/\rho_1} \coth kH_1\right]^{-1}.$$

In figure 3 the internal wave phase and group speeds (ω_-/k and $d\omega_-/dk$) are plotted against wavenumber, for a fresh water layer (density $\rho_1 = 998$ kg m^{-3}) of depth $H_1 = 5$ m above a salt water layer (density $\rho_2 = 1024$ kg m^{-3}) to a total depth $H_2 = 350$ m as before. With $|\rho_2-\rho_1| \ll \rho_1, \rho_2$ the phase and group speeds of the internal waves are significantly less than those of the surface flexural waves. The gravity-dominant character of the internal waves is also apparent, as the group speed decreases more rapidly than the phase speed from a common maximum attained in the long wavelength limit ($k \to 0$) - viz. $g(1 - \rho_1/\rho_2)(H_2 - H_1)H_1/H_2$. Differentiating this expression with respect to H_1, we conclude that the internal wave propagation is fastest when $H_1 = \frac{1}{2}H_2$, and this case is also represented in figure 3.

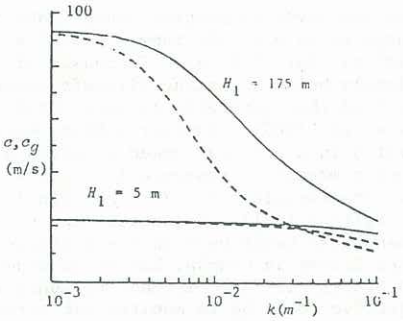

Figure 3. Graphs of phase speed (solid curves) and group speed (dashed curves) for fresh water layer depth H_1 above salt water to 350 m.

4. WAVE PATTERNS

The wave pattern generated depends critically upon vehicle speed. For a steady wave pattern relative to the vehicle, at each point on a wave crest the phase speed must equal the source velocity component normal to the crest - i.e. $c = V\cos\beta$, where β is the angle subtended by the wavenumber vector $\underset{\sim}{k} = (l,m)$ and the constant source velocity $\underset{\sim}{V}$. A vehicle travelling faster than the critical speed c_{min} excites flexural waves in the ice (c.f. figure 1), but a much slower vehicle may excite internal waves in the water. At typical aircraft landing speeds, the flexural wave pattern may exhibit caustics (figure 4a) or a shadow zone (figure 4b). The internal waves are restricted to a triangular region behind the source (figure 5) which narrows as V increases. Note that all these wave patterns were computed for the parameters previously mentioned. Further details may be found in Davys et al. (1985) and Schulkes et al. (1986).

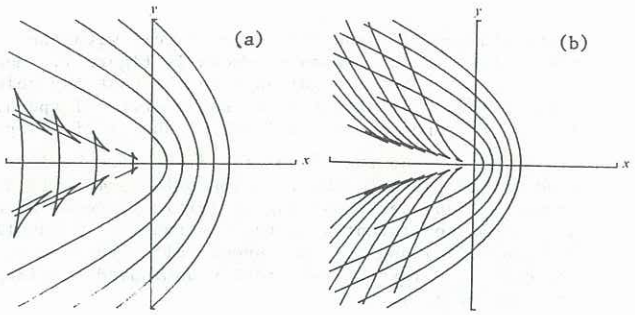

Figure 4. Flexural wavecrest patterns.
(a) V = 50 m/s, with two caustics (two cusps);
(b) V = 60 m/s, with a 'shadow zone' behind the source where no waves appear.

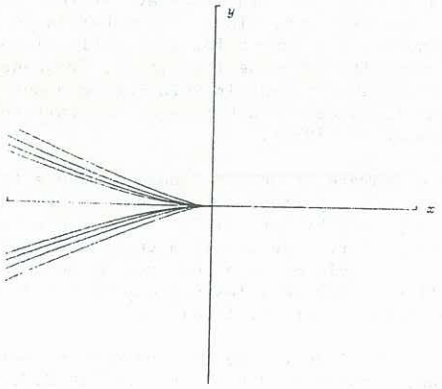

Figure 5. Internal wavecrest pattern for V = 3 m/s (H_1 = 5 m).

5. IMPULSIVELY APPLIED MOVING LINE LOAD

For certain source speeds the wave pattern does not approach a steady state and we must study a time-dependent problem, which can also provide insight into transient behaviour. We neglect water stratification and consider an impulsively applied, steadily-moving concentrated line load

$$f(x,y,t) = F\delta(x - Vt)H(t),$$

where F is the force per unit length, δ the Dirac delta function and H the Heaviside step function. The solution for the ice deflection has been derived by Kheisin (1971) and can be written in the form:

$$\eta(X,t) = \frac{-F}{2\pi\rho}\int_{-\infty}^{\infty}[N_1(k) + N_2(k) - N_3(k)]\tanh(kH)dk, \tag{5.1}$$

where

$$N_1(k) \quad \frac{ke^{ikX}(1 - e^{-i\psi_1 t})}{\psi_1(k)\psi_2(k)}, \qquad N_2(k) = \frac{e^{ikX}e^{-i\psi_1 t}}{2c(k)\psi_2(k)},$$

$$N_3(k) = \frac{e^{ikX}e^{i\psi_2 t}}{2c(k)\psi_2(k)}.$$

Here $\psi_1(k) = k(c - V)$, $\psi_2(k) = k(c + V)$, and $X = x - Vt$ denotes position relative to the source. If the disturbance approaches a steady form, this will be given by

$$\eta_s(X,V) = \int \frac{e^{ikX}}{\psi_1(k)\psi_2(k)}\, k\tanh(kH)dk. \tag{5.2}$$

Note that although the integrand of (5.1) is analytic in some neighbourhood of the real axis, the integrand in (5.2) may have real poles since ψ_1 will have zeros for $V \geq c_{min}$, in which case the contour of integration must be deformed in an appropriate manner. Generally the dominant asymptotic contributions in the limit as $t \to \infty$ are either steady terms arising from zeros of ψ_1, or stationary phase terms of $O(t^{-\frac{1}{2}})$ from zeros of ψ_1'. Since ψ_2 is a monotonically increasing function of k there are no such contributions from $N_3(k)$, which is therefore neglected.

There are two steady regimes demarcated by the critical speed c_{min} = 22.5 m/s (parameters of figure 1).

(i) $V < c_{min}$. In this case ψ_1 has no zeros and ultimately the ice deflection given by (5.2) is static rather than wavelike, because all waves travel faster than the source and radiate away. If $V < c_{gmin}$ there are no points of stationary phase and the transients decay exponentially with time. If $V > c_{gmin}$ there are two points of stationary phase giving transients decaying as $t^{-\frac{1}{2}}$, while if $V = c_{gmin}$ there is a transient decaying as $t^{-1/3}$.

(ii) $V > c_{min}$. If $V < \sqrt{gH}$ = 58.6 m/s, ψ_1 has two real positive zeros, at $k_y < k_z$ say. The steady deflection is (where $c_{gz} = c_g(k_z)$ etc.)

$$\eta_s = \frac{F\tanh(k_z H)}{\rho V(c_{gz} - V)}\sin(k_z X) + R(X), \quad (X > 0),$$

$$= \frac{F\tanh(k_y H)}{\rho V(V - c_{gy})}\sin(k_y X) + R(X), \quad (X < 0),$$

where the term $R(X)$ arising from the purely imaginary zeros of ψ_1 decays exponentially as $X \to \pm\infty$. In essence we have a short-wavelength elastic-dominated wave propagating ahead of the source ($c_{gz} > V$) and a long-wavelength gravity-dominated wave behind ($c_{gy} < V$). There are also two points of stationary phase which give rise to transients decaying as $t^{-\frac{1}{2}}$. When $V > \sqrt{gH}$ the situation is very similar except that only the short-wavelength leading wave is present, since $\sqrt{gH}$ is the maximum possible phase speed for gravity waves.

When the source speed equals c_{min} or $\sqrt{gH}$ however, the deflection does not approach a steady state, unless some energy dissipation is included in the model.

(i) $V = c_{min}$. At the critical speed the two zeros of ψ_1 coalesce with a point of stationary phase, at $k = k_m$ say. The asymptotic form as $t \to \infty$ is

$$\eta = \frac{F\omega_m}{2\rho V k_m}\left[-\cos(k_m X + \pi/4)\left(\frac{t}{t_m}\right)^{\frac{1}{2}} + |k_m X|\cos(k_m X) + \alpha\sin(k_m|X|)\right] + R(X), \tag{5.3}$$

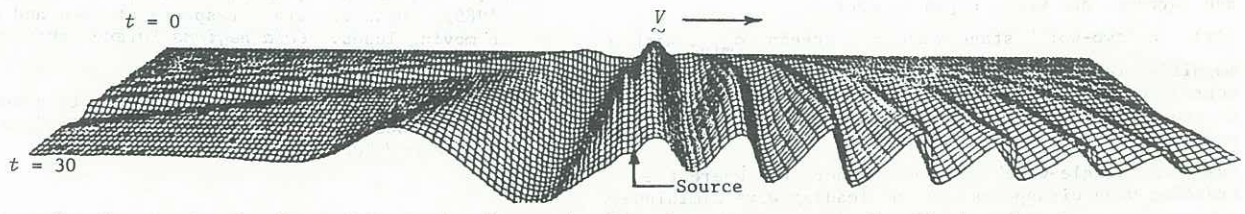

Figure 6. Wave system development from t = 0 to t = 30s for source speed V = 30 m/s otherwise.

where $\omega(k) = \tanh(kH)(k - k_m)^2/\psi_1$, the timescale $t_m = 2\pi/k_m^2 c_{gm}'$, and $\alpha = k_m w_m''/\omega_m$. The most striking feature is that the displacement grows in time as $t^{\frac{1}{2}}$ (c.f. Kheisin 1971). The physical explanation is that the source speed coincides with the wave energy propagation speed - i.e. $V = c_{min} = c_{gm}$. Thus at the critical speed the energy accumulates continuously in the vicinity of the source, the energy density will grow linearly with time, and the deflection as $t^{\frac{1}{2}}$ (c.f. Davys et al. 1985).

(ii) $V = \sqrt{gH}$. Now two points of stationary phase coincide with a zero of ψ_1 at $k = 0$, and the asymptotic form as $t \to \infty$ is

$$\eta = \frac{F\tanh(k_z H)}{\rho V(c_{gz} - V)} \sin(k_z X) + \frac{F}{\rho V^2}\left[\beta\left(\frac{t}{t_0}\right)^{1/3} - \frac{X}{H}\right] + R(X), \qquad (X > 0),$$

$$= \frac{F}{\rho V^2}\left[\beta\left(\frac{t}{t_0}\right)^{1/3} + \frac{2X}{H}\right] + R(X), \qquad (X < 0),$$

where $\beta = \sqrt{3}\Gamma(1/3)/2\pi$, and $t_0 = (H/g)^{\frac{1}{2}}$. We again have $V = c = c_g$ *but only in the limit* $\lambda = 2\pi/k \to \infty$, and the rate of growth is somewhat slower.

We can also illustrate the time-dependence of the deflection by computing it directly from (5.1) by fast Fourier transform. Figure 6 shows results for V = 30 m/s, and the development of the leading and trailing waves can be clearly seen. The group speed of the leading wave relative to the source $(c_g - V)$ is 30.5 m/s and the wavelength is 138 m, so over a period of 30s about 7 wavelengths have been generated. By contrast, the relative group speed of the trailing wave is 14.2 m/s and its wavelength is 571 m, so only one wavelength has been generated over the same period. For *sub-critical* speeds $(V < c_{min})$ the steady ice deflection is shown in figure 7.

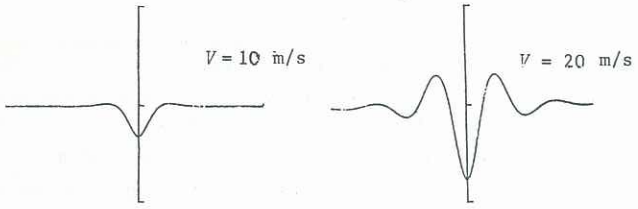

Figure 7. Steady ice deflection at sub-critical speeds.

6. OBSERVATIONS

Whilst the early authors associated critical speed c_{min} with both magnified ice response and the transition to an elastic-gravity wavelike form, quite recent experimental work using deflectometers by Eyre (1977), Beltaos (1980) and Takizawa (1985) has defined five flexural modes, depending on source speed: viz.

(i) a "quasi-static" mode at small V, with ice deflection identical to the static case;

(ii) a "symmetric" or "early" transition stage at larger $V < c_{min}$, where the ice depression below the load deepens and narrows, and an outer rim rises above the neutral ice position;

(iii) an "asymmetric" or "late" transition stage as V approaches c_{min}, when the depression further deepens and narrows, and waves begin to emerge;

(iv) a "two-wave" stage when V exceeds c_{min}, with a magnified response including the narrowest and deepest depression near the source close to critical speed, and generally shorter waves ahead and longer waves behind; and

(v) a "single-wave" stage at higher V, where the trailing wave disappears and the leading wave diminishes.

It is also noticeable that the depression lags further behind the load as V increases.

Flexural modes (i) and (ii) compare well with the theoretical steady responses shown in figure 7. Modes (iii) and (iv) are recognisable in the unsteady solution, which figure 6 illustrates for super-critical speed. A similar response was obtained for sub-critical speed $V = 13\ \mathrm{ms}^{-1}$, and the lag of the depression behind the load was not so noticable. Asymptotic formula (5.3) predicts a quarter-phase lag at critical speed, which also seems consistent with the observations. Wavelike responses (iv) and (v) correspond well with theory, including the loss of the gravity-dominated trailing wave for $V > \sqrt{gH}$.

We also remark that the discrepancy reported between the long trailing wave branch of the theoretical dispersion curve and recent data in the paper by Squire et al. (1985), is consistent with the small relative group speed at which the trailing-wave system propagates - c.f. also figure 6. The strainmeter is an effective alternative instrument for observational work. By analysing its response (amplitude, frequency, phase), we may be able to obtain information about the strength of the ice sheet even before an aircraft touches down (Davys et al. 1985).

We are unaware of observational evidence for internal waves, except perhaps the suggestion of a hydrodynamic wake reported by Eyre (1977), who used a "suspended" deflectometer. Presumably a vehicle moving above the ice sheet could be detected from below however, and relatively slow vehicles may experience an anomalous drag (Schulkes et al. 1986).

We are much indebted to the insight and enthusiasm of two graduate students, J.W. Davys and R.M.S.M. Schulkes, who collaborated in this work.

REFERENCES

BELTAOS, S. (1981): Field studies on the response of floating ice sheets to moving loads. *Can. J. Civil Eng.* Vol. 8(1), 1.

DAVYS, J.W., HOSKING, R.J. & SNEYD, A.D. (1985): Waves due to a steadily moving source on a floating ice plate. *J. Fluid Mech.* Vol. 158, 269.

EYRE, D. (1977): The flexural motions of a floating ice sheet induced by moving vehicles. *J. Glaciol.* Vol. 19, 555.

GREENHILL, A.G. (1887): Wave motion in hydrodynamics. *Am. J. Math.* Vol. 9, 62.

KHEISIN, D.YE. (1971): Some non-stationary problems of dynamics of the ice cover. In *Studies in Ice Physics and Ice Engineering* (ed. Iakolev). Israel Program for Scientific Translations.

LAMB, H. (1945): *Hydrodynamics.* Dover.

LEWIS, E.L. & WALKER, E.R. (1970): The water structure under a growing ice sheet. *J. Geophys. Res.* Vol. 75, 33, 6836.

NEVEL, D.E. (1970): Moving loads on a floating ice sheet. *U.S. Army CRREL Res. Rep.* 261.

SCHULKES, R.M.S.M., HOSKING, R.J. & SNEYD, A.D. (1986): Waves due to a steadily moving source on a floating ice plate II. *Univ. Waikato Math. Res. Rep.* 147.

SQUIRE, V.A., ROBINSON, W.H., HASKELL, T.G. & MOORE, S.C. (1985): Dynamic strain response of lake and sea ice to moving loads. *Cold Regions Science and Technology* Vol. 11, 123.

TAKIZAWA, T. (1985): Deflection of a floating sea ice sheet induced by a moving load. *Cold Regions Science and Technology* Vol. 11, 171.